



Visual spatial attention enhances the amplitude of positive and negative fMRI responses to visual stimulation in an eccentricity-dependent manner

David W. Bressler^{a,b}, Francesca C. Fortenbaugh^{b,c,d}, Lynn C. Robertson^{b,c,d,e}, Michael A. Silver^{a,b,e,*}

^a School of Optometry, University of California, Berkeley, CA 94720, USA

^b Henry H. Wheeler Jr. Brain Imaging Center, University of California, Berkeley, CA 94720, USA

^c Veterans Administration, Martinez, CA 94553, USA

^d Department of Psychology, University of California, Berkeley, CA 94720, USA

^e Helen Wills Neuroscience Institute, University of California, Berkeley, CA 94720, USA

ARTICLE INFO

Article history:

Available online 3 April 2013

Keywords:

Attention

fMRI

Eccentricity

Retinotopy

ABSTRACT

Endogenous visual spatial attention improves perception and enhances neural responses to visual stimuli at attended locations. Although many aspects of visual processing differ significantly between central and peripheral vision, little is known regarding the neural substrates of the eccentricity dependence of spatial attention effects. We measured amplitudes of positive and negative fMRI responses to visual stimuli as a function of eccentricity in a large number of topographically-organized cortical areas. Responses to each stimulus were obtained when the stimulus was attended and when spatial attention was directed to a stimulus in the opposite visual hemifield. Attending to the stimulus increased both positive and negative response amplitudes in all cortical areas we studied: V1, V2, V3, hV4, VO1, LO1, LO2, V3A/B, IPS0, TO1, and TO2. However, the eccentricity dependence of these effects differed considerably across cortical areas. In early visual, ventral, and lateral occipital cortex, attentional enhancement of positive responses was greater for central compared to peripheral eccentricities. The opposite pattern was observed in dorsal stream areas IPS0 and putative MT homolog TO1, where attentional enhancement of positive responses was greater in the periphery. Both the magnitude and the eccentricity dependence of attentional modulation of negative fMRI responses closely mirrored that of positive responses across cortical areas.

© 2013 Elsevier Ltd. All rights reserved.

1. Introduction

Visual attention facilitates processing of the vast amount of information that bombards our eyes. In the spatial domain, visual target detection is improved at attended locations and impaired at unattended locations (Bashinski & Bacharach, 1980; Posner, Snyder, & Davidson, 1980). Spatial attention can also counteract the reduction in perceptual performance caused by external noise (Lu, Lesmes, & Doshier, 2002) or distractors surrounding the target (Zenger, Braun, & Koch, 2000). Physiologically, spatial attention increases activity in portions of retinotopic visual cortical maps that represent the attended location (Gandhi, Heeger, & Boynton, 1999; Kastner et al., 1999; McAdams & Maunsell, 1999; Treue & Martínez Trujillo, 1999) and suppresses activity in cortex that represents unattended locations (Müller & Kleinschmidt, 2004; Silver, Ress, & Heeger, 2007; Tootell et al., 1998).

* Corresponding author. Address: 360 Minor Hall, University of California, Berkeley, CA 94720-2020, USA. Fax: +1 510 643 5109.

E-mail address: masilver@berkeley.edu (M.A. Silver).

The properties of visual processing vary widely across the visual field. Visual acuity and contrast sensitivity are significantly worse for peripheral compared to central vision (reviewed in Kitterle (1986)), as is performance on visual search tasks (Carrasco et al., 1995). In contrast, temporal processing is better (Carrasco et al., 2003; Hartmann, Lachenmayr, & Brettel, 1979), and surround suppression (Xing & Heeger, 2000) and crowding (Bouma, 1970) are stronger for peripheral compared to central vision. Early visual cortical areas contain an expanded representation of the central visual field, known as cortical magnification (Fishman, 1997; Horton & Hoyt, 1991; Schira, Wade, & Tyler, 2007). However, scaling the size of visual stimuli for peripheral locations based on this cortical magnification factor eliminates some but not all reported eccentricity-dependent psychophysical effects (Carrasco & Frieder, 1997; Kitterle, 1986).

Despite substantial evidence for differences in visual processing between central and peripheral vision, less is known regarding eccentricity-dependent effects of spatial attention. Presentation of an exogenous cue enhances visual acuity for targets subsequently presented at the cued location, and this attentional enhancement is greater for peripheral compared to central target

locations in both humans (Yeshurun & Carrasco, 1999) and monkeys (Golla et al., 2004). Visual search exhibits a similar eccentricity profile of attention effects, with larger beneficial effects of exogenous cues for more peripheral targets (Carrasco & Yeshurun, 1998).

The eccentricity dependence of the effects of attention on perception can also depend on task. For tasks that benefit from improved spatial resolution at all eccentricities, enhancement of performance by an exogenous attention cue increases as a function of eccentricity (Carrasco, Williams, & Yeshurun, 2002). However, for a texture segmentation task in which heightened resolution is expected to impair performance at near eccentricities, exogenous attention improves performance at far eccentricities and worsens it at near eccentricities (Yeshurun & Carrasco, 1998, 2000), consistent with exogenous attention increasing spatial resolution for all eccentricities. On the other hand, endogenous attention improves texture segmentation performance at all eccentricities (Yeshurun, Montagna, & Carrasco, 2008), suggesting that endogenous attention can either increase or decrease spatial resolution, depending on task demands (Carrasco, 2011).

One way that attention may improve perceptual spatial resolution is by decreasing neuronal receptive field (RF) size. In V1, endogenous spatial attention reduces excitatory RF size for neurons at near eccentricities ($2\text{--}3^\circ$) but increases RF size for neurons at more peripheral eccentricities ($6\text{--}7^\circ$) (Roberts et al., 2007). These eccentricity-dependent effects of attention on RF size result in greater attentional modulation of response amplitude for smaller stimuli at more central visual field locations and for larger stimuli at more peripheral locations. Although these findings are important in demonstrating eccentricity dependence of the neural correlates of attentional modulation in V1, only two eccentricities were examined in this study. In addition, the eccentricity profile of attentional modulation is unknown in areas outside of V1 and has not been investigated at all in the human brain.

We used fMRI to measure the effects of endogenous visual spatial attention on the amplitude of positive and negative visual responses in many topographically-organized cortical areas in human occipital and parietal cortex. Attention substantially increased both positive and negative response amplitudes in all cortical areas. However, we found that the effects of attention varied as a function of eccentricity and that this eccentricity dependence differed across cortical areas. Specifically, early visual, ventral, and lateral occipital cortical areas showed greater attentional enhancement of positive response amplitude at near compared to far eccentricities, possibly reflecting a role for endogenous attention in resolving fine detail of an attended object in central vision. In contrast, posterior parietal area IPS0 and temporal occipital area TO1 showed greater attentional enhancement of positive response magnitude at far compared to near eccentricities, perhaps reflecting

the importance of detecting behaviorally relevant objects in the periphery for planning of motor responses. Finally, the magnitudes of attentional modulation of positive and negative responses were highly correlated across brain areas, and a similar correlation across brain areas was observed for eccentricity dependence of attentional modulation of positive and negative responses.

2. Material and methods

2.1. Subjects

Nine healthy subjects (2 males, 7 females) participated in the study, all of whom had extensive experience as subjects in psychophysical and fMRI experiments. Two subjects (F.C.F., M.A.S) were also authors of the study. All participants provided written informed consent, and the experimental protocol was approved by the Committee for the Protection of Human Subjects at the University of California, Berkeley. Each subject participated in one session to acquire high-resolution whole-brain anatomical MRI images and in one retinotopic mapping fMRI session. Prior to the retinotopic mapping session, each subject practiced the target detection task for a total of two hours in a behavioral testing room, allowing subject performance to reach asymptotic levels. In addition, behavioral data from the practice sessions were used to determine the target sizes for each subject that resulted in equivalent performance across eccentricities in the fMRI experiment.

2.2. Visual stimuli and task

Stimuli were presented using an LCD projector (Avotec, Stuart, FL). A circular grid was visible on the screen at all times during fMRI scanning (Fig. 1). The grid was divided into 12 wedges, each of which subtended 30° , and 6 rings, each of which had a width of 3° of visual angle, for a total of 72 patches. The 6 rings were at eccentricities of $0.5\text{--}3^\circ$, $3\text{--}6^\circ$, $6\text{--}9^\circ$, $9\text{--}12^\circ$, $12\text{--}15^\circ$, and $15\text{--}18^\circ$ of visual angle. A fixation point with radius of 0.2° of visual angle was displayed at the center of the grid.

At any point in time, each patch was either ON (containing a checkerboard with checks that changed color at 5 Hz) or OFF (isoluminant gray). For each trial, one patch in the left visual field and one patch in the right visual field were ON, and the rest of the patches were OFF (Fig. 1). Luminance contrast of the checkerboard was always at least 65%. The actual luminance values varied slightly, as checks were randomly assigned either dark or light colors (Fig. 1), with the constraint that no check could be either white (maximal luminance) or black (minimal luminance) (Swisher et al., 2007). Each check subtended 10° of polar angle (i.e., 36 checks arranged in a ring shape would cover all visual field locations at a

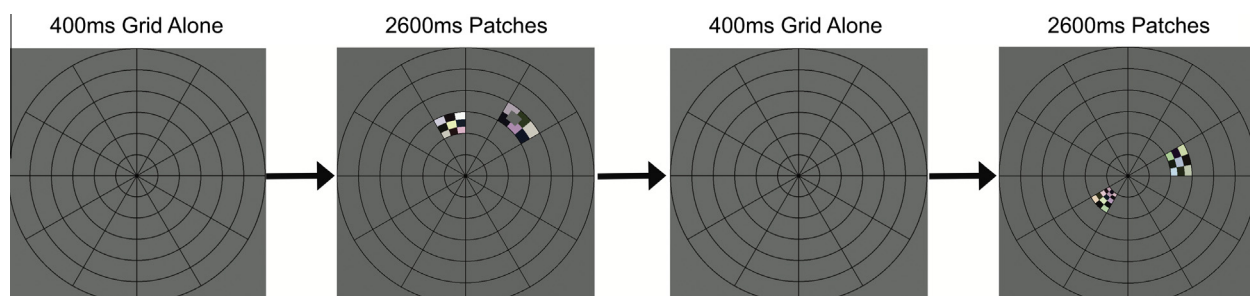


Fig. 1. Two example trials. Subjects maintained fixation while viewing a circular stimulus grid. Each trial began with 400 ms of grid presentation. During the remaining 2600 ms, colorful contrast-reversing checkerboard patterns were simultaneously presented in one patch on each side of the grid. Subjects attended to the patches on the left or right side on alternating runs and reported when a low-contrast target was presented within the attended patch. In this example, a target was presented on the first trial but not the second trial.

given eccentricity), and the range of eccentricities contained within each check was scaled according to the cortical magnification factor in human V1 (Slotnick et al., 2001). The checkerboard pattern was presented only in patches within the four inner rings of the grid, for a total of 48 patch locations (2 visual hemifields \times 6 polar angles \times 4 eccentricities) that were visually stimulated over the course of each run.

The beginning of each run started with 3 s (1 TR) of blank screen, followed by 9 s of presentation of only the circular grid. For each of the subsequent 192 TRs (576 s), there was a trial during which the checkerboard pattern was presented in two patch locations (one in the left and one in the right visual field) (Fig. 1). Each run ended with 18 s of circular grid presentation, for a total of 606 s (202 TRs) per run. On average, a given patch contained a visual stimulus once every 72 s, for a total of 8 stimulus presentations per patch for each run. The sequence of ON and OFF states for each patch was determined by randomly generating 10,000 stimulus presentation sequences for the set of 24 patch locations in each hemifield, with the constraint that all 24 patch locations had to be stimulated in succession before a stimulus could be presented again at a given patch location. The stimulus sequence within this set of 10,000 random sequences that had the lowest temporal correlation between spatial patterns of visual stimulation (specifically, minimal kurtosis of the distribution of correlation coefficients) was then selected for the experiments.

At the beginning of each trial, the luminance of the fixation point briefly increased for 100 ms to remind subjects to maintain central fixation. After an additional 300 ms (during which only the grid and fixation point were presented), the checkerboard pattern appeared in two patches for 2600 ms (Fig. 1). On a given run, subjects were instructed to detect targets within the ON patch in either the left or right visual field while maintaining fixation at a central point. The target was a briefly presented (200 ms) gray annular segment (i.e., similar shape as the patches) of zero contrast with mean luminance equal to that of the checkerboard stimulus. The target subtended 10° of polar angle (equal to the size of one check along this dimension), and the range of eccentricities contained within the target was determined for each participant prior to testing in order to achieve approximately 80–85% correct trials at all eccentricities. The mean eccentricity of the target was the same as the mean eccentricity of the patch in which it was presented. The target could appear on either the left or right side of the patch, with the center of the target offset one-half check from the left or right edge of the patch. Thus, the target was superimposed on multiple checks and had sharp luminance edges that were displaced relative to the edges of the checks (Fig. 1). The target appeared with 50% probability within each ON patch with an onset time ranging from 400 to 2400 ms after the onset of the patch.

To equate sensory stimulation in the attend-left and attend-right conditions, contrast decrement targets were presented within the ON patches in both the left and right hemifields (although the temporal sequences of presentation in the left and right visual hemifields were independent and were based on a 50% probability of presentation for each trial). Subjects pressed a button whenever they detected the target in the ON patch in the attended visual field. If necessary, the sizes of the targets were adjusted between runs during the fMRI experiments to maintain approximately equivalent performance for each of the eccentricity rings. The attend-left and attend-right runs always occurred consecutively in pairs, and any changes to the target sizes during the experiment were applied to both runs in the pair. In addition, the sequence of stimulus presentation was the same for a given pair of runs, so identical visual stimuli were shown for attend-left and attend-right conditions. Thus, the only difference between the two attention conditions was the side of the visual field that subjects

attended. Five subjects attended to the left visual field during the first scan, and the remaining four subjects attended to the right visual field during the first scan.

2.3. fMRI data acquisition

Functional MRI experiments were conducted with a 3 Tesla Siemens Trio MR scanner. A transmit/receive radiofrequency coil was used to maximize contrast-to-noise ratio in posterior cortex. Functional echo-planar images were acquired using a gradient-echo sequence. The field of view was 200×200 mm, and the matrix size was 78×78 , resulting in an inplane voxel resolution of 2.6×2.6 mm. The repetition time (TR) was 3000 ms, and the echo time (TE) was 24 ms. Twenty-seven slices were prescribed with an interslice gap of 0.25 mm and a slice thickness of 2.5 mm. The slices were angled between the coronal and axial planes to provide coverage of occipital and posterior parietal cortex. A set of T1-weighted anatomical images that were coplanar with the EPI images was acquired at the beginning of every imaging session. Each run lasted 606 s (202 TRs), and each subject completed either 8 or 10 runs.

2.4. fMRI data preprocessing

Head movements were corrected offline using a 3D image registration algorithm (MCFLIRT; Jenkinson et al., 2002). The time series from each run were concatenated across runs of a given attention condition (attend-left or attend-right), so that a voxel's concatenated time series for a given attention condition was either 808 TRs (4 runs) or 1010 TRs (5 runs) long. Each of these two concatenated time series for each voxel was divided by its mean intensity to convert the data from arbitrary units to percent signal modulation and to compensate for the decrease in mean image intensity as a function of distance from the radiofrequency coil. Finally, both time series were high-pass filtered above 0.014 Hz in each voxel.

2.5. Estimation of visual fMRI responses for each patch location

To determine the locations and boundaries of topographically-organized cortical areas, we averaged the BOLD response at each voxel across the attend-left and attend-right conditions (the sequence of visual stimulation was identical for these two conditions). For each voxel, we then used reverse correlation to estimate its BOLD response to visual stimulation at each patch location (Hansen, David, & Gallant, 2004; Hansen, Kay, & Gallant, 2007). A strength of this reverse correlation procedure is that it does not require any assumptions regarding the shape of the hemodynamic response. The kernel of the BOLD response, $h(\tau)$, is derived from the cross-correlation of a particular voxel's fMRI time series data $R(t)$ and the time-offset stimulus sequence at a particular patch $S(t - \tau)$:

$$h(\tau) = \frac{1}{\sigma_S^2 T} \sum_{t=1}^T R(t)(S(t - \tau) - \bar{S})$$

Here, t is time (in units of TR), σ_S^2 is the variance of the stimulus sequence, T is the total number of TRs, τ is the time lag between the stimulus and the hemodynamic response, S takes values of either 1 (stimulus-ON) or 0 (stimulus-OFF), and \bar{S} is the mean value of S . $h(\tau)$ is in units of percent change in BOLD signal (same units as $R(t)$). The response of a voxel to a given patch was defined as the average of the kernel values at 3 s and at 6 s after stimulus onset. We chose this temporal lag window (overlapping with the rise and peak of the hemodynamic response) because it resulted in more consistent responses than other lag windows.

For each voxel, we performed permutation testing to identify the set of stimulus locations that evoked a significant positive response in that voxel. The sequence of each patch's ON and OFF stimulus time series was randomized, and we computed kernels from the cross-correlations between these randomized sequences of stimulus presentation and the voxel's fMRI time series. This procedure was repeated 500 times for each voxel/patch location combination, and the significance threshold for a positive response in a voxel was defined as the response amplitude greater than 95% of the values produced by this randomization procedure. A patch was considered to elicit a significant negative response in a voxel if the response amplitude was lower than 95% of the values in the permutation distribution. The use of nonparametric permutation testing has the advantage of not requiring any assumptions regarding the shape of the distribution of estimated response magnitudes, and permutation testing with this statistical threshold has previously been used to identify the set of visual field locations that elicit a reliable response from a given voxel (Hansen, David, & Gallant, 2004). On average, there were six patches with significant positive responses and six patches with significant negative responses per voxel (i.e., across voxels, an average of 36 of 48 patches did not evoke a significant response).

The resulting set of patch locations in the visual field that generated a significant positive response in a given voxel is the response profile for that voxel. We next computed the center of mass of this positive response profile for each voxel (in visual field coordinates). For each voxel, the polar angle value of its response to each patch was calculated by generating a vector with an angle equal to that of the location of the patch in visual space and a length scaled by the amplitude of the response generated by a visual stimulus within that patch. The length of vectors for patches with responses that fell below the positive significance threshold was set to zero. This resulted in 48 vectors, one per patch, and the center of the response profile for each voxel was defined as the polar angle of the sum of these vectors.

A similar procedure was used to compute the eccentricity of the center of the positive response profile. We first scaled the eccentricity of each patch by the positive response amplitude generated by a visual stimulus within that patch (setting the response amplitude of patches with non-significant positive responses to zero), summed these scaled values across all 48 locations, and divided this by the sum of all significant response amplitudes. The resulting weighted-average eccentricity value assigned to each voxel was a continuous variable bounded by the center of the most foveal patch location (1.5°) and the center of the most peripheral patch location (10.5°) in the stimulus array.

We used the angle and eccentricity values computed from the average of the attend-left and attend-right time series for each voxel to define visual field boundaries between adjacent mirror-image visual field representations for early (V1–V3), ventral (human V4 (hV4), VO1), lateral occipital (LO1, LO2), temporal occipital (TO1, TO2), and dorsal occipital (V3A/B, IPS0) cortical areas (Figs. 2 and 3). The boundaries of VO2 and of posterior parietal topographic areas beyond IPS0 were not clearly defined in many hemispheres, so we have excluded these areas from our analyses.

For every stimulus patch, there were an equal number of runs during which spatial attention was focused on the patch and other runs in which spatial attention was directed to a patch in the opposite hemifield. For each voxel and patch combination, we used the reverse correlation procedure described above to compute attended and unattended response amplitudes. For a given voxel, the positive response amplitude corresponded to the mean response across all patches that evoked a significant positive response in the average of the attend-left and attend-right time series. An analogous procedure was used to compute negative response amplitude. Attentional modulation of response amplitude

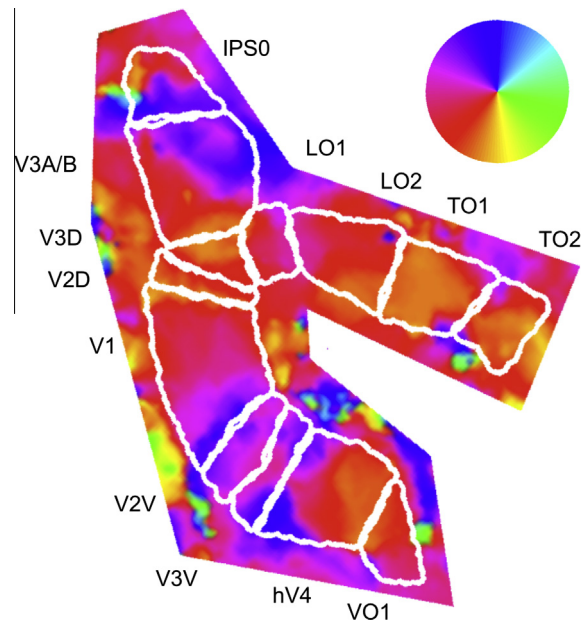


Fig. 2. Angular component of visual field locations superimposed on flattened patch of right posterior cortex from an example subject. For each voxel, an average time series was computed from an equal number of attend-left and attend-right runs. Reverse correlation was used to determine the set of visual field locations that produced a significant positive response in each voxel. The centers of mass of these positive response profiles were transformed into polar visual field coordinates and visualized on computationally-flattened patches of occipital and parietal cortex. The color wheel indicates the one-to-one mapping between each cortical location and the angular component of the corresponding visual field location. In this cortical patch from the right hemisphere, each topographic area represents the contralateral left visual field.

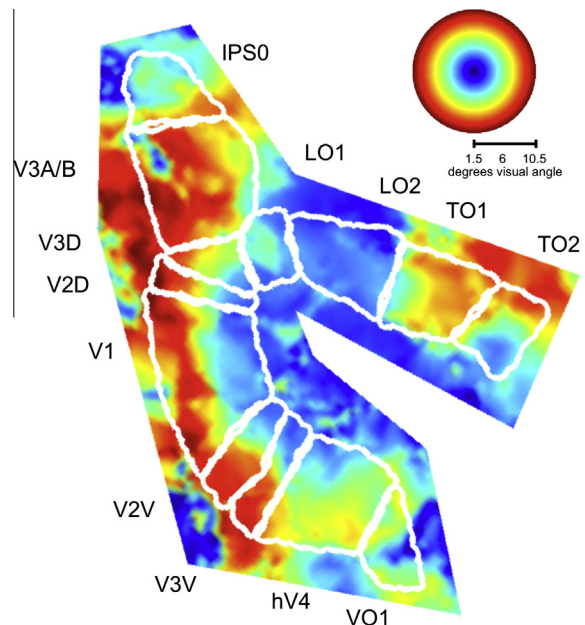


Fig. 3. Representations of visual field eccentricity in topographically-organized areas in occipital and parietal cortex. Data and conventions are the same as in Fig. 2, but eccentricity is displayed instead of polar angle.

was then expressed as a percentage of the response amplitude in the average time series ($100 * ((\text{attended} - \text{unattended}) / \text{average})$) for both positive and negative fMRI responses, weighted by the average response for both attention conditions. We corrected for

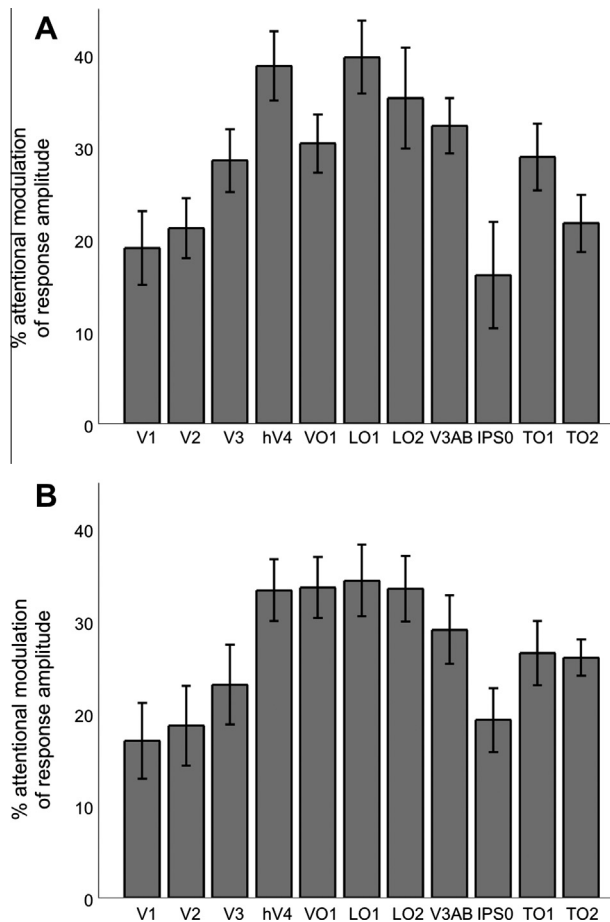


Fig. 4. Attentional enhancement of positive and negative response amplitudes. (A) Attending to the visual stimulus significantly increased the amplitude of the positive stimulus-evoked response in every topographically-organized area that was studied. (B) Attending to the stimulus also increased the amplitude of the negative BOLD response to the stimulus in all areas. Note that an enhancement of the amplitude of the negative response by attention is plotted as positive attentional modulation here and in subsequent figures.

multiple statistical comparisons for the eleven cortical areas using the false discovery rate (FDR) method (Genovese, Lazar, & Nichols, 2002).

We quantified eccentricity dependence by fitting a linear function to the plot of attentional modulation of response amplitude versus eccentricity in each cortical area and each subject, with each voxel contributing a single data point to this plot. The slope of the linear fit quantifies the eccentricity dependence of the attentional modulation. For graphical display (Fig. 5), we averaged attention modulation values across all voxels with eccentricities centered in each of nine eccentricity bands (1–2°, 2–3°, 3–4°, 4–5°, 5–6°, 6–7°, 7–8°, 8–9°, and 9–10° of visual angle), excluding the most eccentric band (10–11°).

3. Results

3.1. Behavioral results

Subjects maintained fixation while checkerboard stimuli were simultaneously presented within single patches in the left and right sides of a stimulus array. Gray targets were presented within the stimulated patches with 50% probability for each patch presentation, and subjects were instructed on alternating runs (approximately 10 min in duration) to detect a target within the checkerboard patch in either the left (attend-left condition) or

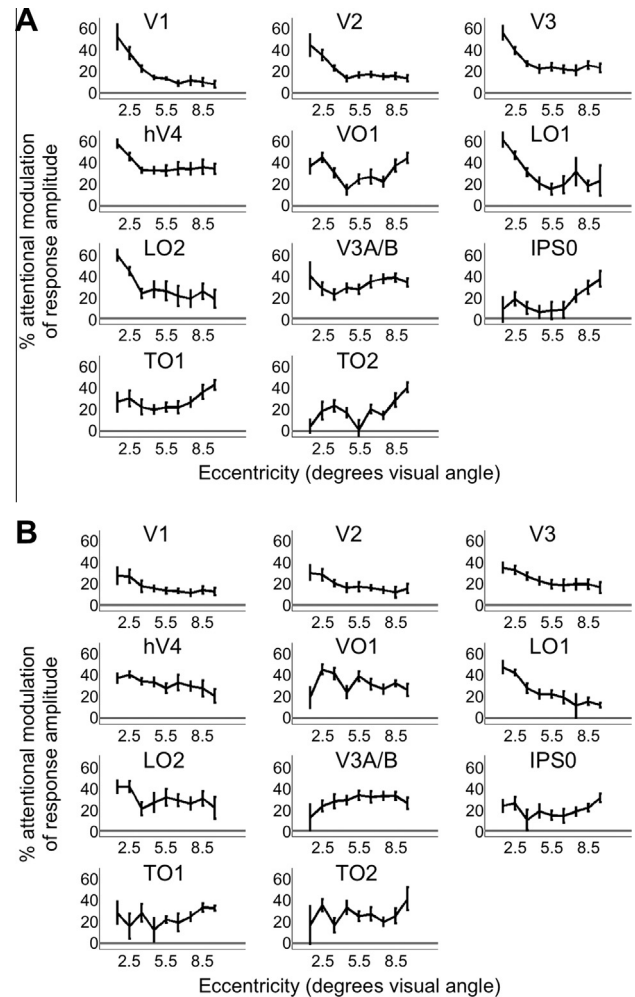


Fig. 5. Eccentricity dependence of attentional modulation of positive and negative response amplitudes. (A) For positive responses, attention increased response amplitude more for near than far eccentricities in areas V1, V2, V3, hV4, LO1, and LO2. In areas IPS0 and TO1, attentional enhancement of positive responses was greater for far compared to near eccentricities. (B) For negative responses, attention increased response amplitude more for near than far eccentricities in areas V1, V2, V3, hV4, LO1, and LO2.

right (attend-right condition) visual field (Fig. 1). Target sizes were selected to produce equivalent behavioral performance (approximately 80–85% correct trials) for targets at each eccentricity.

There was no significant group difference in overall performance (percent correct trials) between the attend-left and attend-right conditions ($p = 0.13$, two-tailed paired t -test, $n = 9$ subjects). In addition, there was no significant group difference in performance between attend-left and attend-right conditions for any single eccentricity band (0.5–3°: $p = 0.16$; 3–6°: $p = 0.24$; 6–9°: $p = 0.10$; 9–12°: $p = 0.99$, two-tailed paired t -test, $n = 9$ subjects). The fact that performance was equivalent for attend-left and attend-right conditions controls for a number of possible confounds, including differences in fMRI responses due to task difficulty, attentional effort, or arousal.

The percentage of correct trials did not systematically vary across the four eccentricity bands (0.5–3°: 80%; 3–6°: 87%; 6–9°: 82%; 9–12°: 86%). To formally test for a systematic relationship between target eccentricity and behavioral performance, we fit a linear function to the plot of percent correct trials versus eccentricity band for each subject. The mean of the slope values from these linear fits was not significantly different from zero ($p = 0.11$). False alarm rates were low across all subjects and eccentricity bands,

comprising an average of 3% of all trials. We also conducted all analyses of percent correct trials described above on d' values and obtained similar results: no significant difference between attend-left and attend-right trials ($p = 0.64$) and no detectable relationship between target eccentricity and d' ($p = 0.06$).

3.2. Topographic mapping

For each voxel, we determined the set of patch locations within the stimulus array that evoked a statistically significant positive fMRI response. The center of the positive response profile (in visual field coordinates; based on the average of attend-left and attend-right conditions) was computed for each voxel and was used to generate polar angle (Fig. 2) and eccentricity (Fig. 3) maps of visual field locations. Based on these maps, we were able to define the boundaries of topographically-organized areas V1, V2, V3, human V4 (hV4), VO1, LO1, LO2, V3A/B, IPS0, TO1, and TO2 in both hemispheres of all nine subjects.

3.3. Spatial attention increases positive and negative response amplitudes in an eccentricity-dependent manner

For each voxel in each cortical area, we calculated the average response amplitude separately for attended and unattended conditions. Positive responses were averaged across all patch locations that evoked a significant positive response in the average of the attend-left and attend-right time series. Attentional modulation was defined as the difference in positive response in attended and unattended conditions, normalized by the mean positive response amplitude in the average time series of the two attention conditions. Directing spatial attention to a stimulus significantly increased mean positive response amplitude in all cortical areas (Fig. 4A; $p < 0.05$, two-tailed t -test, $n = 9$ subjects, FDR-corrected for multiple comparisons), with attentional enhancement ranging from approximately 15% to 40%.

We quantified the eccentricity dependence of this effect by fitting a linear function to the plot of attentional modulation of positive response amplitude versus eccentricity in each cortical area and each subject, with each voxel contributing a single data point. Attention enhanced positive response amplitude more for near than far eccentricities (i.e., slope of linear fit was significantly less than zero) in early visual cortical (V1–V3), ventral (hV4), and lateral occipital (LO1 and LO2) cortical areas ($p < 0.05$, two-tailed t -test, $n = 9$ subjects, FDR-corrected) (Fig. 5A). In contrast, attention enhanced positive responses more for far than for near eccentricities in dorsal stream cortical areas IPS0 and putative MT homolog TO1 (i.e., slope of linear fit was significantly greater than zero; $p < 0.05$, two-tailed t -test, $n = 9$ subjects, FDR-corrected) (Fig. 5A). Note that for visualization purposes, data were binned by eccentricity in Fig. 5.

In topographically-organized cortical areas, visual stimuli often evoke a positive fMRI response in cortical locations that represent the visual field location of the stimulus and a negative fMRI response in regions that represent surrounding unstimulated visual field locations (Shmuel et al., 2002; Silver, Shenhav, & D'Esposito, 2008). We measured the amplitude of negative fMRI responses and found that attention significantly increased the strength of these responses (i.e., made the response more negative) in all cortical areas ($p < 0.05$, two-tailed t -test, $n = 9$ subjects, FDR-corrected) (Fig. 4B), with attentional modulation values ranging from approximately 15% to 35%. Attentional modulation of negative responses was significantly greater for near than far eccentricities in areas V1, V2, V3, hV4, LO1, and LO2 (i.e., slope of the linear fit was significantly less than zero; $p < 0.05$, two-tailed t -test, $n = 9$ subjects, FDR-corrected) (Fig. 5B). Note that an increase in negative

response amplitude is plotted as positive attentional modulation in Figs. 4B, 5B, and 6.

If response reliability varied as a function of eccentricity, this could have influenced the measurement of eccentricity dependence of attentional modulation. For example, if the SNR of responses to the checkerboard patch stimuli was lower in the periphery than in central visual field locations in a given brain area, this could have made it more difficult to detect attentional modulation in the periphery in that area, as the estimates of responses to attended and unattended stimuli would have been less reliable at these locations. We directly tested this possibility by convolving the time series of stimulus presentation at each patch with the corresponding kernel (derived from the reverse correlation procedure), thereby creating a model time series for every voxel. We then measured response reliability by computing the mean squared error (MSE) between this model time series and the measured fMRI time series for each voxel. For each cortical area, we

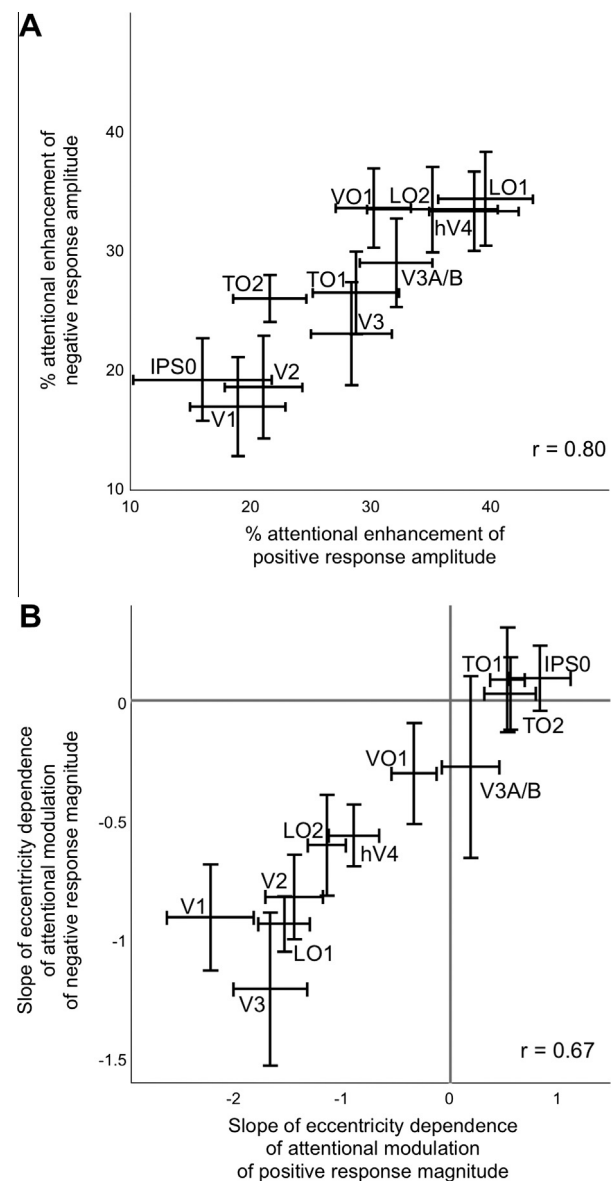


Fig. 6. Correlation of attentional enhancement of positive and negative responses. (A) The magnitudes of attentional enhancement of positive and of negative responses were highly correlated across cortical areas. (B) The eccentricity dependence (mean slope of the linear fits of the attentional modulation versus eccentricity plots) was highly correlated for positive and negative responses across cortical areas.

then generated scatter plots of MSE versus eccentricity, with each voxel contributing one data point, and tested for eccentricity dependence of MSE in the same way we tested for eccentricity dependence of attentional modulation. No cortical area had a statistically significant FDR-corrected p -value (i.e., mean slope of linear fits was not significantly different from zero), indicating that the eccentricity dependence of attentional modulation of positive and negative responses (Fig. 5) cannot be accounted for by eccentricity dependence of response reliability.

3.4. Attentional enhancement of positive and negative responses is positively correlated across cortical areas

We correlated the magnitude of attentional enhancement of positive and negative responses across cortical areas and found a significant positive correlation ($r = 0.80$; $p < 0.05$, two-tailed t -test, $n = 9$ subjects) (Fig. 6A). A similar analysis of the slopes of the linear fits of the attentional modulation versus eccentricity plots for positive and negative responses also revealed a significant positive correlation ($r = 0.67$; $p < 0.05$, two-tailed t -test, $n = 9$ subjects) (Fig. 6B).

4. Discussion

4.1. Eccentricity dependence of effects of spatial attention on positive responses to visual stimuli

We found that directing endogenous attention to a visual stimulus substantially enhanced the amplitude of the positive response to that stimulus in every topographic cortical area we studied. This enhancement of visual cortical response amplitude by spatial attention is consistent with previous results obtained with single-unit recordings in macaque (McAdams & Maunsell, 1999; Treue & Martínez Trujillo, 1999) and with fMRI in humans (Buracas & Boynton, 2007; Gandhi, Heeger, & Boynton, 1999).

The eccentricity dependence of this amplification of positive response amplitude by spatial attention varied across areas. In early visual cortex (V1–V3) and ventral area hV4, RF sizes at the eccentricities stimulated in the current experiment are relatively small, facilitating perception of fine spatial detail. In these areas, attention enhanced positive response amplitude more for near than far eccentricities. Similar results were obtained in lateral occipital areas LO1 and LO2. Therefore, our results show that in early visual, ventral, and lateral occipital cortex, attention had the largest effect on positive response amplitude for central visual field locations where perceptual spatial resolution is finest. At peripheral eccentricities where perceptual resolution is poor, attention had smaller effects in early visual, ventral, and lateral occipital cortex. This pattern of results is consistent with a role for endogenous attention in facilitating the processing of fine spatial detail in central vision.

However, behavioral studies of exogenous attention have consistently reported greatest benefits at more eccentric locations (Carrasco & Yeshurun, 1998; Carrasco, Williams, & Yeshurun, 2002; Golla et al., 2004; Yeshurun & Carrasco, 1998; Yeshurun & Carrasco, 2000). These results have generally been interpreted as an enhancement of perceptual spatial resolution by exogenous attention. The finding of improved texture segmentation performance at all eccentricities following an endogenous attention cue can also be understood as a change in spatial resolution (Yeshurun, Montagna, & Carrasco, 2008), with attention decreasing resolution at more central locations and increasing it at more peripheral locations, based on the demands of the task. One possible neurophysiological mechanism of increased perceptual spatial resolution is a reduction in neuronal RF size. However, endogenous attention reduces V1 neuronal RF size at central visual field locations and

increases RF size at peripheral visual field locations in macaque monkeys (Roberts et al., 2007). This eccentricity dependence of attention effects on a neural measure of spatial resolution seems inconsistent with the behavioral findings, in which attention increases spatial resolution in the periphery.

While our findings clearly show greatest attentional enhancement of fMRI response amplitude for central locations in early visual, ventral, and lateral occipital cortex, it is difficult at this time to directly relate these effects of attention to those on neuronal RF size and perceptual spatial resolution (for a review of behavioral and neurophysiological measures of attentional modulation of spatial resolution, see Anton-Erxleben & Carrasco, 2013). It is possible that an increase in neural and/or perceptual spatial resolution would be accompanied by an increase in the spatial resolution of fMRI responses. However, the relationship between changes in spatial resolution of fMRI responses and changes in the amplitude of fMRI responses is not completely understood. Administration of the cholinesterase inhibitor donepezil reduced excitatory fMRI response amplitude to visual stimulation in early visual cortex but increased the spatial resolution of these responses (Silver, Shenhav, & D'Esposito, 2008), while another study showed that endogenous spatial attention increased the amplitude as well as the spatial resolution of fMRI responses in early visual cortex (Fischer & Whitney, 2009). Recent advances in methods to directly estimate spatial tuning of fMRI responses in visual cortex (Dumoulin & Wandell, 2008; Fischer & Whitney, 2009; Silver, Shenhav, & D'Esposito, 2008) will be useful for characterizing the effects of attention on both spatial resolution and response amplitude, thereby clarifying the relationships between these two physiological measures and how each of them correlates with the effects of attention on behavior.

In posterior parietal cortical area IPS0 and temporal occipital area TO1, endogenous attention increased positive response amplitude more for peripheral than central stimulus locations. Area IPS0, originally known as V7, contains a topographic map of visual spatial attention signals (Tootell et al., 1998). Area TO1 has been proposed to be the human homolog of macaque area MT (Amano, Wandell, & Dumoulin, 2009), and regions within the intraparietal sulcus and the human MT⁺ complex have been identified as components of the dorsal cortical attention network (Fox et al., 2005; Vincent et al., 2006). An important function of the dorsal cortical attention network is identification of spatial locations as targets for subsequent shifts in voluntary attention and eye position (Corbetta & Shulman, 2002). Therefore, the larger effects of attention that we observed for peripheral representations in IPS0 and TO1 may be related to the dorsal attention system's role in shifting the locus of endogenous spatial attention. The selective attentional enhancement of peripheral representations we observed in IPS0 and TO1 may promote more effective detection of behaviorally relevant objects in the periphery that can then be brought into foveal vision for more detailed analysis. This would be consistent with behavioral results showing perceptual enhancement for stimuli at a location that has been identified as a target for an upcoming saccade, even before the saccade is initiated (Harrison, Mattingley, & Remington, 2013; Rolfs & Carrasco, 2012; Zhao, Gersch, Schnitzer, Doshier, & Kowler, 2012).

4.2. Visual spatial attention increases negative responses to visual stimulation

In early visual cortex, visual stimulation evokes both a positive fMRI response in regions that retinotopically represent the stimulated visual field locations and a surrounding negative fMRI response in regions that represent adjacent unstimulated locations (Shmuel et al., 2002; Silver, Shenhav, & D'Esposito, 2008; Tootell et al., 1998). A number of findings suggest that negative BOLD responses to visual stimulation have a neural basis and are not

simply due to “blood stealing”, in which oxygenated blood is diverted from less active to more active neighboring tissue. In primary visual cortex, negative BOLD responses are accompanied by a reduction in neuronal firing rate (Shmuel et al., 2006), and negative BOLD responses occur in the hemisphere of visual cortex that is ipsilateral to the stimulus location (Smith, Williams, & Singh, 2004; Tootell et al., 1998). Additionally, negative BOLD responses in early visual cortex contain precise information about visual stimulus location (Bressler, Spotswood, & Whitney, 2007).

In the present study, attention enhanced the amplitude of the negative fMRI response to the visual stimulus in every area we studied. Similar results have been previously described in primary visual cortex (Heinemann, Kleinschmidt, & Müller, 2009; Müller & Kleinschmidt, 2004; Smith, Singh, & Greenlee, 2000). Here we extend these findings by showing that substantial attentional modulation of negative fMRI responses is present in a large number of areas in ventral, temporal, lateral, and dorsal occipital cortex. In our study, only a small portion of the visual field contained a visual stimulus, so most if not all of the negative BOLD responses were in cortical regions representing unstimulated visual field locations. This is consistent with a previous study showing that sustained spatial attention in the absence of visual stimulation induces negative BOLD activity in portions of early visual cortex that represent unattended visual field locations (Silver, Ress, & Heeger, 2007).

4.3. Eccentricity dependence of effects of spatial attention on negative responses to visual stimuli

We observed a significant effect of eccentricity on attentional enhancement of negative fMRI responses in cortical areas V1, V2, V3, hV4, LO1, and LO2, with these areas exhibiting greater effects of attention at near compared to far eccentricities. This set of areas is identical to that identified as having the same eccentricity profile of attentional enhancement of positive responses. However, the greater attentional enhancement of positive responses for far compared to near eccentricities in IPS0 and TO1 was not observed for negative responses. This may be related to the relatively large RF sizes in these areas. The spatial spread of positive fMRI responses to visual stimuli is greater in IPS0 than in early visual cortical areas (Tootell et al., 1998), consistent with larger neuronal excitatory RF sizes in IPS0 compared to early visual cortex. Similarly, spatial tuning of individual voxel responses is weaker in TO1 compared to early visual cortex and LO1 and LO2 (Amano, Wandell, & Dumoulin, 2009; Henriksson et al., 2012). For voxels with large RFs, those that are centered in the outer eccentricity bands of our stimulus array will be likely to have more of their inhibitory surround region located outside (more peripheral to) the stimulus array, compared to voxels at more central visual field locations. Because we did not include responses to visual field locations outside the stimulus array in our analyses, negative responses in these locations did not contribute to our estimates of attentional modulation. This could have reduced the measured attentional modulation of negative responses of IPS0 and TO1 voxels at peripheral eccentricities compared to more central eccentricities, thereby masking a possible eccentricity dependence of attention effects on negative responses (specifically, attentional modulation greater for far than near eccentricities) that was detectable in positive responses in these areas. Additional studies employing a larger stimulus array are needed to more definitively address these questions.

Nevertheless, the eccentricity profile of the effects of spatial attention on negative responses closely mirrored that of positive responses (i.e., the slopes of lines fitted to attentional modulations of negative and positive responses across eccentricities were highly correlated) (Fig. 6B). This suggests that for a given cortical area, enhancement of positive responses at attended locations and negative responses at unattended locations could serve similar

functions. In areas exhibiting stronger attention effects at central compared to peripheral eccentricities, increases in both positive and negative responses could reflect greater “contrast” between center and surround portions of RFs, leading to improved response reliability (Bressler & Silver, 2010) and/or enhanced processing of fine spatial detail (Roberts et al., 2007).

4.4. Possible effects of eye movements

Eye movements were not recorded during the fMRI experiments. However, it is unlikely that deviations from fixation could account for any of our findings. First, all subjects were experienced psychophysical observers, and seven of nine subjects had previous extensive practice in covert attention tasks requiring sustained central fixation. Second, significant deviations from fixation would have limited our ability to map visual field representations of topographically-organized cortical areas, yet we defined the locations and boundaries of V1, V2, V3, hV4, VO1, LO1, LO2, V3A/B, IPS0, TO1, and TO2 in both hemispheres of all participants. Finally, our finding of qualitatively different patterns of eccentricity dependence of attentional modulation in different cortical areas is inconsistent with a global effect of eye movements on the eccentricity dependence of fMRI responses to visual stimulation.

5. Conclusions

We have shown that modulation of the amplitude of both positive and negative fMRI responses to visual stimuli by endogenous spatial attention is strongly dependent on eccentricity. In early visual, ventral, and lateral occipital cortex, attention increased positive responses evoked by a visual stimulus more in central than in peripheral visual field locations. This eccentricity dependence is consistent with a facilitatory role of spatial attention in processing of fine spatial detail of objects at central visual field locations. In contrast, attentional enhancement of positive stimulus-evoked responses was greater for peripheral than central visual field locations in cortical areas IPS0 and TO1. Greater attentional enhancement at peripheral locations in these areas may be useful for identifying behaviorally relevant locations in the periphery to guide saccadic and other motor responses to these locations. Finally, attentional enhancement of negative BOLD responses was highly correlated with the corresponding enhancement of positive responses across areas. These correlations were observed both for the magnitude of attentional enhancement (collapsed across eccentricities) as well as for the eccentricity dependence of the effects of attention. In addition to providing important descriptive information regarding the effects of spatial attention across visual field representations in a large number of cortical areas, our findings establish a foundation for characterizing brain/behavior correlations that will yield a better understanding of the neural bases of performance differences in central and peripheral vision.

Acknowledgments

This research was supported by the Chancellor's Faculty Partnership Fund at the University of California, Berkeley (M.A.S. and L.C.R.), National Science Foundation Graduate Research Fellowships (D.W.B. and F.C.F.), the Veterans Administration, and NEI Core Grant EY003176. The authors thank Natalie Pierson for assistance in drawing boundaries of cortical visual field maps.

References

- Amano, K., Wandell, B. A., & Dumoulin, S. O. (2009). Visual field maps, population receptive field sizes, and visual field coverage in the human MT+ complex. *Journal of Neurophysiology*, 102, 2704–2718.

- Anton-Erxleben, K., & Carrasco, M. (2013). Attentional enhancement of spatial resolution: linking behavioural and neurophysiological evidence. *Nature Reviews Neuroscience*, 14, 188–200.
- Bashinski, H. S., & Bacharach, V. R. (1980). Enhancement of perceptual sensitivity as the result of selectively attending to spatial locations. *Perception & Psychophysics*, 28, 241–248.
- Bouma, H. (1970). Interaction effects in parafoveal letter recognition. *Nature*, 226, 177–178.
- Bressler, D. W., & Silver, M. A. (2010). Spatial attention improves reliability of fMRI retinotopic mapping signals in occipital and parietal cortex. *Neuroimage*, 53, 526–533.
- Bressler, D., Spotswood, N., & Whitney, D. (2007). Negative BOLD fMRI response in the visual cortex carries precise stimulus-specific information. *PLoS ONE*, 2, e410.
- Buracas, G. T., & Boynton, G. M. (2007). The effect of spatial attention on contrast response functions in human visual cortex. *Journal of Neuroscience*, 27, 93–97.
- Carrasco, M. (2011). Visual attention: the past 25 years. *Vision Research*, 51, 1484–1525.
- Carrasco, M., Evert, D. L., Chang, I., & Katz, S. M. (1995). The eccentricity effect: target eccentricity affects performance on conjunction searches. *Perception & Psychophysics*, 57, 1241–1261.
- Carrasco, M., & Frieder, K. S. (1997). Cortical magnification neutralizes the eccentricity effect in visual search. *Vision Research*, 37, 63–82.
- Carrasco, M., McElree, B., Denisova, K., & Giordano, A. M. (2003). Speed of visual processing increases with eccentricity. *Nature Neuroscience*, 6, 699–700.
- Carrasco, M., Williams, P. E., & Yeshurun, Y. (2002). Covert attention increases spatial resolution with or without masks: support for signal enhancement. *Journal of Vision*, 2, 467–479.
- Carrasco, M., & Yeshurun, Y. (1998). The contribution of covert attention to the set-size and eccentricity effects in visual search. *Journal of Experimental Psychology: Human Perception and Performance*, 24, 673–692.
- Corbetta, M., & Shulman, G. L. (2002). Control of goal-directed and stimulus-driven attention in the brain. *Nature Reviews Neuroscience*, 3, 201–215.
- Dumoulin, S. O., & Wandell, B. A. (2008). Population receptive field estimates in human visual cortex. *Neuroimage*, 39, 647–660.
- Fischer, J., & Whitney, D. (2009). Attention narrows position tuning of population responses in V1. *Current Biology*, 19, 1356–1361.
- Fishman, R. S. (1997). Gordon Holmes, the cortical retina, and the wounds of war. *Documenta Ophthalmologica*, 93, 9–28.
- Fox, M. D., Snyder, A. Z., Vincent, J. L., Corbetta, M., Van Essen, D. C., & Raichle, M. E. (2005). The human brain is intrinsically organized into dynamic, anticorrelated functional networks. *Proceedings of the National Academy of Sciences USA*, 102, 9673–9678.
- Gandhi, S. P., Heeger, D. J., & Boynton, G. M. (1999). Spatial attention affects brain activity in human primary visual cortex. *Proceedings of the National Academy of Sciences USA*, 96, 3314–3319.
- Genovese, C. R., Lazar, N. A., & Nichols, T. (2002). Thresholding of statistical maps in functional neuroimaging using the false discovery rate. *Neuroimage*, 15, 870–878.
- Golla, H., Ignashchenkova, A., Haarmeier, T., & Thier, P. (2004). Improvement of visual acuity by spatial cueing: a comparative study in human and non-human primates. *Vision Research*, 44, 1589–1600.
- Hansen, K. A., David, S. V., & Gallant, J. L. (2004). Parametric reverse correlation reveals spatial linearity of retinotopic human V1 BOLD response. *Neuroimage*, 23, 233–241.
- Hansen, K. A., Kay, K. N., & Gallant, J. L. (2007). Topographic organization in and near human visual area V4. *Journal of Neuroscience*, 27, 11896–11911.
- Harrison, W. J., Mattingley, J. B., & Remington, R. W. (2013). Eye movement targets are released from visual crowding. *Journal of Neuroscience*, 33, 2927–2933.
- Hartmann, E., Lachenmayr, B., & Brettel, H. (1979). The peripheral critical flicker frequency. *Vision Research*, 19, 1019–1023.
- Heinemann, L., Kleinschmidt, A., & Müller, N. G. (2009). Exploring BOLD changes during spatial attention in non-stimulated visual cortex. *PLoS ONE*, 4, e5560.
- Henriksson, L., Karvonen, J., Salminen-Vaparanta, N., Railo, H., & Vanni, S. (2012). Retinotopic maps, spatial tuning, and locations of human visual areas in surface coordinates characterized with multifocal and blocked fMRI designs. *PLoS ONE*, 7, e36859.
- Horton, J. C., & Hoyt, W. F. (1991). The representation of the visual field in human striate cortex: a revision of the classic Holmes map. *Archives of Ophthalmology*, 109, 816–824.
- Jenkinson, M., Bannister, P., Brady, M., & Smith, S. (2002). Improved optimization for the robust and accurate linear registration and motion correction of brain images. *Neuroimage*, 17, 825–841.
- Kastner, S., Pinsk, M. A., De Weerd, P., Desimone, R., & Ungerleider, L. G. (1999). Increased activity in human visual cortex during directed attention in the absence of visual stimulation. *Neuron*, 22, 751–761.
- Kitterle, F. L. (1986). Psychophysics of lateral tachistoscopic presentation. *Brain and Cognition*, 5, 131–162.
- Lu, Z. L., Lesmes, L. A., & Doshier, B. A. (2002). Spatial attention excludes external noise at the target location. *Journal of Vision*, 2, 312–323.
- McAdams, C. J., & Maunsell, J. H. R. (1999). Effects of attention on orientation-tuning functions of single neurons in macaque cortical area V4. *Journal of Neuroscience*, 19, 431–441.
- Müller, N. G., & Kleinschmidt, A. (2004). The attentional 'spotlight' penumbra: center-surround modulation in striate cortex. *Neuroreport*, 15, 977–980.
- Posner, M. I., Snyder, C. R., & Davidson, B. J. (1980). Attention and the detection of signals. *Journal of Experimental Psychology: General*, 109, 160–174.
- Roberts, M., Delicato, L. S., Herrero, J., Gieselmann, M. A., & Thiele, A. (2007). Attention alters spatial integration in macaque V1 in an eccentricity-dependent manner. *Nature Neuroscience*, 10, 1483–1491.
- Rolfs, M., & Carrasco, M. (2012). Rapid simultaneous enhancement of visual sensitivity and perceived contrast during saccade preparation. *Journal of Neuroscience*, 32, 13744–13752.
- Schira, M. M., Wade, A. R., & Tyler, C. W. (2007). Two-dimensional mapping of the central and parafoveal visual field to human visual cortex. *Journal of Neurophysiology*, 97, 4284–4295.
- Shmuel, A., Augath, M., Oeltermann, A., & Logothetis, N. K. (2006). Negative functional MRI response correlates with decreases in neuronal activity in monkey visual area V1. *Nature Neuroscience*, 9, 569–577.
- Shmuel, A., Yacoub, E., Pfeuffer, J., Van de Moortele, P. F., Adriany, G., Hu, X., & Ugurbil, K. (2002). Sustained negative BOLD, blood flow and oxygen consumption response and its coupling to the positive response in the human brain. *Neuron*, 36, 1195–1210.
- Silver, M. A., Ress, D., & Heeger, D. J. (2007). Neural correlates of sustained spatial attention in human early visual cortex. *Journal of Neurophysiology*, 97, 229–237.
- Silver, M. A., Shenhav, A., & D'Esposito, M. (2008). Cholinergic enhancement reduces spatial spread of visual responses in human early visual cortex. *Neuron*, 60, 904–914.
- Slotnick, S. D., Klein, S. A., Carney, T., & Sutter, E. E. (2001). Electrophysiological estimate of human cortical magnification. *Clinical Neurophysiology*, 112, 1349–1356.
- Smith, A. T., Singh, K. D., & Greenlee, M. W. (2000). Attentional suppression of activity in the human visual cortex. *Neuroreport*, 11, 271–277.
- Smith, A. T., Williams, A. L., & Singh, K. D. (2004). Negative BOLD in the visual cortex: evidence against blood stealing. *Human Brain Mapping*, 21, 213–220.
- Swisher, J. D., Halko, M. A., Merabet, L. B., McMains, S. A., & Somers, D. C. (2007). Visual topography of human intraparietal sulcus. *Journal of Neuroscience*, 27, 5326–5337.
- Tootell, R. B. H., Hadjikhani, N., Hall, E. K., Marrett, S., Vanduffel, W., Vaughan, J. T., & Dale, A. M. (1998). The retinotopy of visual spatial attention. *Neuron*, 21, 1409–1422.
- Treue, S., & Martínez Trujillo, J. C. (1999). Feature-based attention influences motion processing gain in macaque visual cortex. *Nature*, 399, 575–579.
- Vincent, J. L., Snyder, A. Z., Fox, M. D., Shannon, B. J., Andrews, J. R., Raichle, M. E., & Buckner, R. L. (2006). Coherent spontaneous activity identifies a hippocampal-parietal memory network. *Journal of Neurophysiology*, 96, 3517–3531.
- Xing, J., & Heeger, D. J. (2000). Center-surround interactions in foveal and peripheral vision. *Vision Research*, 40, 3065–3072.
- Yeshurun, Y., & Carrasco, M. (1998). Attention improves or impairs visual performance by enhancing spatial resolution. *Nature*, 396, 72–75.
- Yeshurun, Y., & Carrasco, M. (1999). Spatial attention improves performance in spatial resolution tasks. *Vision Research*, 39, 293–306.
- Yeshurun, Y., & Carrasco, M. (2000). The locus of attentional effects in texture segmentation. *Nature Neuroscience*, 3, 622–627.
- Yeshurun, Y., Montagna, B., & Carrasco, M. (2008). On the flexibility of sustained attention and its effects on a texture segmentation task. *Vision Research*, 48, 80–95.
- Zenger, B., Braun, J., & Koch, C. (2000). Attentional effects on contrast detection in the presence of surround masks. *Vision Research*, 40, 3717–3724.
- Zhao, M., Gersch, T. M., Schnitzer, B. S., Doshier, B. A., & Kowler, E. (2012). Eye movements and attention: The role of pre-saccadic shifts of attention in perception, memory and the control of saccades. *Vision Research*, 74, 40–60.